View metadata, citation and similar papers at core.ac.uk

brought to you by CORE

provided by NASA Technical Reports Server

IN-27

129299

P.22

NASA Technical Memorandum

NASA TM-108379

GLASS FIBER PROCESSING FOR THE MOON/MARS PROGRAM
(Center Director's Discretionary Fund Final Report)

By D.S. Tucker, E. Ethridge, and P. Curreri

Materials and Processes Laboratory
Science and Engineering Directorate

October 1992

(NASA-TM-108379) GLASS FIBER PROCESSING FOR THE MOON/MARS PROGRAM: CENTER DIRECTOR'S DISCRETIONARY FUND FINAL REPORT (NASA) 22 p

N93-13115

Unclas

G3/27 0129299

National Aeronautics and Space Administration

George C. Marshall Space Flight Center

ACKNOWLEDGMENTS

The authors would like to acknowledge Mr. Guy Smith and Dr. Gary Workman of the University of Alabama in Huntsville for their work in construction of the fiber pulling apparatus.

TABLE OF CONTENTS

	Page
INTRODUCTION	1
EXPERIMENTAL METHODS AND RESULTS	1
Materials	1
Fiber Processing	2
Fiber Pulling Apparatus Description	3
FPA Results	3
DISCUSSION	4
CONCLUSIONS	4
REFERENCES	6

ii INTENTIONALLY BLANK

PRECEDING PAGE BLANK NOT FILMED

LIST OF ILLUSTRATIONS

Figure	Title	Page
1.	MLS–1 DTA curve	9
2.	MLS–1 glass DTA curve	9
3.	DTA curve for vitrified MLS–2	10
4.	MLS–1 viscosity curve	10
5.	MLS–2 viscosity curve	11
6.	E-glass viscosity curve	11
7.	Comparison of MLS–1 and MLS–2 viscosities	12
8.	Schematic of laboratory fiber pulling unit	12
9.	Continuously wound MLS–2 fiber doped with 8 percent B_2-O_3	13
10.	MLS–2 fiber doped with 8 percent B_2-O_3. Fiber diameter is 80 microns	13
11.	Schematic of fiber pulling apparatus	14
12.	Schematic of FPA data acquisition system	14
13.	Fiber jet zones during parabolic maneuver	15
14.	Concept for quenching glass fiber	16

LIST OF TABLES

Table	Title	Page
1.	Major element chemistry of MLS–1	7
2.	Summary of compositions of starting materials for MLS–2	8

TECHNICAL MEMORANDUM

GLASS FIBER PROCESSING FOR THE MOON/MARS PROGRAM
(Center Director's Discretionary Fund Final Report)

INTRODUCTION

With NASA's commitment to a permanent manned presence in low-Earth orbit (LEO) (Space Station *Freedom*) and eventual return to the Moon, numerous studies have been undertaken in the areas of microgravity and lunar materials processing.[1,2] Continuous glass fiber processing is one such area of research interest. In LEO, processing of optical and single crystal fibers may be enhanced due to the absence of gravity forces.[3] In fact, a miniaturized fiber pulling apparatus (FPA) for drawing single-crystal core glass fibers in LEO has been developed.[4] On the lunar surface, abundant materials exist which can be used to produce structural materials. The use of lunar regolith for the production of structural materials could greatly reduce the cost of construction and long-term habitation of a lunar colony. One lunar product, fiberglass (both continuous and discontinuous forms) promises ease of manufacture and wide applicability.[5] Continuous fiberglass can be utilized as reinforcement in structural composites, including pressure vessels, glass cables, and woven-fiber insulation. The chemistry of lunar soils is similar to that of terrestrial basalts.[6,7] Terrestrial basalt has been used to produce continuous glass fiber, with chemical and mechanical properties similar to that of E-glass.[8,9] Comparable glass fibers have been produced with simulated basalt.[10] This report describes research which was undertaken to study the production of continuous glass fiber from two lunar soil simulants.

An important part of this study involved determining the effects of lunar gravity on fiber formation. An FPA was constructed and parabolas were flown on NASA's KC–135 aircraft to simulate lunar gravity.

EXPERIMENTAL METHODS AND RESULTS

Materials

The materials used in this study are known as "Minnesota Lunar Simulant–1" (MLS–1)* and "Minnesota Lunar Simulant–2" (MLS–2).* MLS–1 is a low-titanium basalt similar in chemistry to that of Apollo sample 10084.[11] The results of elemental analysis of MLS–1 and Apollo sample 10084 are given in table 1. The grain size of MLS–1 is similar to coarser lunar mare basalts (<1 mm) but is more equigranular, perhaps due to recrystallization.[11] Lunar soils generally contain varying amounts of glass and agglutinates due to micrometeorite impact.[12] MLS–1 contains 10 to 30 weight percent glass products produced by processing in an in-flight sustained shockwave plasma reactor (ISSP).[11] This compares to 10 to 80 weight percent found in lunar soil samples.

*University of Minnesota Space Sciences Laboratory.

MLS–2 is a highlands simulant containing more silica and less titania than MLS–1. It also contains a great deal more alumina. Average starting compositions of MLS–2 are given in table 2. Differential thermal analysis (DTA) was used to characterize each simulant and the glasses processed from each. The melting point was determined to be 1,200 °C for MLS–1 (fig. 1). This was confirmed by heating a small amount of MLS–1 in a platinum boat to 1,200 °C in a tube furnace and observing the material. Glassy MLS–1 was made by firing the simulant to 1,450 °C for 24 h in a box furnace, then pouring the melt onto an aluminum block. This material was crushed and DTA performed. The result is shown in figure 2. The exotherm noted at approximately 1,125 °C could be interpreted as recrystallization of the basalt material.

The DTA trace for the MLS–2 yields a more complex situation. There is no clear evidence of distinct melting, but rather peaks indicating reactions and possible polymorphic transformations. DTA of glassy MLS–2 prepared in the identical manner as MLS–1 yields a trace with three exotherms and one endotherm (fig. 3). The exotherms likely represent recrystallization, while the endotherm may be due to structural transformation of recrystallized material.

Viscosity measurements (Theta Industries, Port Washington, NY) of the MLS–1 and MLS–2 yielded the curves shown in figures 4 and 5, respectively. The curves are plotted as log viscosity (viscosity in poise (P)) versus temperature in degrees centigrade. A curve for E-glass is shown as reference in figure 6. This curve was plotted from tabulated viscosity data.[13] As can be seen from figure 4, the viscosity of MLS–1 does not evidence the gradual decrease in viscosity with temperature as does the E-glass. This implies there is little or no glass working range to MLS–1. A comparative plot between MLS–1 and MLS–2 is shown in figure 7. In this case, viscosity in centipoise versus temperature is plotted. It can be seen from this plot that the MLS–2 has a higher viscosity at higher temperatures and a gentler slope. This would imply a more stable working range.

Fiber Processing

In order to produce continuous fibers of MLS–1 and MLS–2, the apparatus shown in figure 8 was constructed. The apparatus consists of a platinum-wound furnace containing a single-hole platinum bushing, a power supply, and a takeup reel. The furnace is mounted on a tripod approximately 2 ft above the takeup reel. The takeup reel is driven by an ordinary laboratory stirring motor. Vitrified simulant is placed into the bushing through the top of the furnace and heated to a temperature which allows fiber spinning. Fiber spinning is begun by hand drawing the fiber from the bushing orifice to the takeup reel using an alumina rod. Fiber is wound continuously until the bushing is empty of simulant.

Only short fiber segments were pulled from MLS–1. Ideal viscosity for fiber pulling is approximately 10,000 P. For MLS–1, this viscosity lies well below the melting point and within recrystallization range. In fact, it was found that the simulant would recrystallize in the bushing below 1,205 °C. At this temperature and above, the molten simulant would run freely from the bushing orifice. This agrees with the viscosity data in figure 4. The fiber segments which were successfully pulled evidenced small crystallites visible under a low-power microscope.

Longer segments of MLS–2 could be pulled; however, the same type of problems associated with the MLS–1 occurred as well. In order to enhance the viscosity range of the MLS–2, 8 weight percent B_2-O_3 was added to the raw simulant. Boric oxide is a glass former with low viscosity as compared to other glass-forming oxides.[14] However, B_2-O_3 shows anomalous viscosity behavior when mixed with glass modifiers. That is, the viscosity increases with additions of modifiers rather than

decreases as is seen with silicon dioxide. This has been attributed to change in the coordination number of oxygen with boron.[14] Vitrified material was made in the same manner as the two raw simulants. The doped simulant was pulled continuously at 1,300 °C. An example of the wound fiber package is shown in figure 9. Fiber as small as 30 μm in diameter was produced. A typical segment from a wound package is shown in figure 10. Evidence of recrystallization was not observed using optical microscopy. Additions of B_2-O_3 to the MLS–1 did not enhance fiber pulling behavior.

Twenty-eight specimens from the fiber package were cut to 4-in lengths and tested for tensile strength. The average specimen diameter was 45 μm. The mean strength was 60,000 lb/in^2 with a standard deviation of 17,500 lb/in^2. To increase fiber strength, B_2-O_3-doped MLS–2 fiber was produced with a polyvinyl alcohol sizing. The sizing was a 5-percent aqueous solution. The sizing was applied by pulling the fiber between two saturated pieces of felt. Each piece of felt was attached to a reservoir of polyvinyl alcohol solution. A hot-air gun was directed onto the fiber to dry the sizing before winding on the spindle. Thirty-eight samples were tested for breaking strength. Average fiber diameter was measured to be 30 μm. The mean strength was 102,000 lb/in^2 with a standard deviation of 40,000 lb/in^2. For comparison, E-glass fiber can have strengths as high as 500,000 lb/in^2.

FPA Description

The FPA was constructed to study the effects of lunar gravity on fiber formation. This apparatus was flown onboard the KC–135 aircraft. Referring to figure 11, the FPA consists of a furnace containing a single-orifice platinum bushing and temperature controller, a takeup reel and winding motor, a video camera, a quench plate, and a heat exchanger. These components are enclosed in a Plexiglas box. There is an inlet for dry nitrogen so that the relative humidity of the apparatus can be reduced during fiber drawing. A hygrometer is located on the inside rear wall of the apparatus which reads relative humidity. The FPA is controlled by a data acquisition system. This system consists of an IBM AT personal computer with an eight-channel, 12-bit A/D board, super VHS recorder; electronics for the winding servomotor and furnace; and a TVGA video graphics overlay card (fig. 12).

FPA Results

Ground tests of the FPA were performed using E-glass as the fiber forming material. E-glass is a silica-based glass with well-characterized fiber-forming characteristics. The E-glass was supplied in 25-mm diameter marble form. These marbles were remelted at 1,400 °C for 24 h in a platinum crucible and poured onto an aluminum block to form droplets approximately 10 mm in diameter. The droplets were placed into the FPA furnace and heated to 1,175 °C. Continuous fiber was pulled at varying winding speeds from 30 to 1,000 cm/s.

E-glass was also used during KC–135 flights. The FPA has flown four flights to date with an average of 40 parabolic maneuvers per flight. All maneuvers simulated lunar gravity ($^1/_6$ g). The furnace was heated to 1,175 °C which gave a sample temperature of approximately 1,100 °C. Fiber was continuously pulled throughout each maneuver. During the 2-g portion of the parabola, the fluid jet as it exited the bushing orifice was observed to be 4 mm in diameter at a constant winding speed of 30 cm/s. As g-load was decreased, the fluid jet diameter was seen to decrease steadily to a minimum value of 3 mm at $^1/_6$ g. This affected final fiber diameter as a function of g-load. At $^1/_6$ g, the final fiber diameter was measured to be 100 μm in diameter, at 1 g, 160 μm and 240 μm at 2 g. Figure 13 shows images from the super VHS video tape showing the difference in size of the fluid jet as a function of gravity.

It was found that if the winding speed was increased above 30 cm/s the fiber would break approximately 1 in below the bushing orifice due to attenuation of the fiber jet at 1/6 g. Fiber strength was not tested due to winding abrasion and the variation in fiber diameter due to variable g-loading. Attempts were also made to spin MLS–1 fiber. These attempts were unsuccessful due to recrystallization of the MLS–1 in the bushing.

DISCUSSION

Using E-glass as an ideal glass-fiber forming material, the two raw simulants tested do not compare well. Both exhibit nonglass-like viscosity behavior and a strong tendency to recrystallization when the vitrified materials are heated to below the melting point. Composition, of course, dictates these characteristics. The ability to produce continuous fiber from the B_2-O_3-modified MLS–2 indicates that the composition of this material was adjusted such that recrystallization tendencies were inhibited at the pulling temperature. The higher silica content, along with a lower titania of the as-received MLS–2 as compared to the MLS–1, makes this material a more likely candidate for fiber pulling. Although a viscosity-versus-temperature curve was not produced for this material, an increase in viscosity was observed during the pulling operations as compared to the raw simulants. The strength of the B_2-O_3-doped MLS–2 was seen to increase by approximately 40,000 lb/in^2 when coated. Since glass normally fails from surface flaws, the coating acted to protect the as-spun fiber. It is felt that decreasing the fiber diameter to the 10- to 15-μm range will enhance the strength even more. There was also some evidence of recrystallization in the coated fibers which kept the strength at a lower value. Recrystallized material would act as stress raisers in the fiber.

Although there was little success pulling continuous fibers with the as-received simulants, it is felt that these materials can be made into acceptable fibers. This could be done with appropriate changes in the fiber pulling equipment. One method would be to keep the vitrified simulant a few degrees above the melting temperature and provide a rapid quench to the fiber as it exits the bushing orifice. In effect, one would be freezing an amorphous structure into the fiber before recrystallization has time to occur. This method is shown schematically in figure 14. At some experimentally determined distance below the bushing orifice, a quench plate would be positioned. This quench plate would be a simple annulus through which the fiber would be pulled. It would act as a heat exchanger with flowing, chilled water as the heat transfer medium.

CONCLUSIONS

It was concluded from this study that lunar simulants MLS–1 and MLS–2 in the as-received state were unsuitable for producing continuous glass fibers with the present capabilities. This was attributed to recrystallization near the melting point and a narrow viscosity range from which to pull fibers. Doping MLS–2 with B_2-O_3 yielded a material which could be pulled continuously. This is most likely due to compositional changes resulting in a wider viscosity pulling range and suppression of recrystallization. Breaking strength of doped MLS–2 was increased by coating the fiber with polyvinyl alcohol during the spinning operation. The decrease in fiber diameter from 45 to 30 μm could also account for some of the strength increase.

It is also concluded that MLS–1 and MLS–2 could produce continuous fibers if the appropriate modifications are made to the pulling apparatus.

Lunar gravity was seen to affect fiber formation as evidenced from KC–135 flight data. It was found that at a constant pulling temperature of approximately 1,100 °C, the winding speed could not be raised above 30 cm/s or fiber breakage would occur. This was due to attenuation of the fiber fluid jet during the $^1/_6$-g portion of the maneuver. To the author's knowledge, this phenomenon has not been previously reported.

REFERENCES

1. Proceedings of Lunar Bases and Space Activities of the 21st Century, Washington, DC, 1985.

2. "Materials Processing in the Reduced Gravity Environment of Space," Materials Research Society Proceedings, vol. 87, 1987.

3. Schlicta, P.J., and Nerad, B.A.: "Advantages of Drawing Crystal-Core Fibers in Microgravity." SPIE Proceedings, vol. 1557, 1991.

4. Schlicta, P.J.: "Miniaturized Fiber Pulling Apparatus for Producing Single-Crystal-Core Glass Fibers in Microgravity." Final Report, contract NAS3-25400, 1988.

5. Criswell, D.R.: "Lunar Materials." Second Princeton Conference on Space Manufacturing Facilities-Space Colonies, 1975.

6. McKenzie, J.D., and Claridge, R.C.: "Glass and Ceramics From Lunar Materials." AIAA Proceedings, 1979, pp. 135–140.

7. Allton, J.H., Galindo, C. Jr., and Watts, L.A.: "Guide to Using Lunar Soil and Simulants for Experimentation." Lunar Bases and Space Activities of the 21st Century Proceedings, 1985, p. 497.

8. Chemical and Engineering News, June 4, 1973, p. 49; April 29, p. 18.

9. Subramanian, R.V., Yang, T.J.Y., and Austin, H.F.: "Reinforcement of Polymers by Basalt Fibers." SAMPE Quarterly, July 1977, pp. 1–10.

10. Magoffin, M., and Garvey, J.: "Lunar Glass Production Using Concentrated Solar Energy." AIAA Space Programs and Technological Conference, September 25–28, 1990, Huntsville, AL.

11. Weiblen, P.W., Murawa, M.J., and Reid, K.J.: "Preparation of Simulants for Lunar Surface Materials." Proceedings of Space '90, Aerospace/ASCE/Albuquerque, NM, April 22–26, 1990.

12. Papike, J.J., Hodges, F.N., Bence, A.E., Cameron, M., and Rhodes, J.M.: "Mare Basalts: Crystal Chemistry, Mineralogy, and Petrology." Review of Geophysics and Space Physics, vol. 14(4), 1976, pp. 475–540.

13. Bansal, N.P., and Doremus, R.H. (eds.): "Handbook of Glass Properties," 1986, p. 34.

14. Doremus, R.H.: "Glass Science." John Wiley and Sons, New York, NY, 1973.

Table 1. Major element chemistry of MLS–1.

Percent	Average	Maximum	Minimum
$Si-O_2$	43.86	45.90	41.70
$Ti-O_2$	6.32	7.43	4.82
Al_2-O_3	13.68	15.60	11.76
Fe-O	13.40	14.40	12.00
Fe_2-O_3	2.60	4.10	0.90
Mg-O	6.68	8.44	5.57
Mn-O	0.198	0.218	0.182
Ca-O	10.13	11.48	9.04
Na_2-O	2.12	2.27	1.97
K_2-O	0.281	0.348	0.167
P_2-O_5	0.20	0.45	0.02
CO_2	0.0015	0.0018	0.0014
p/m	**Average**	**Maximum**	**Minimum**
Be	1.00	1.22	0.87
Zn	122	141	97
Cu	445	706	214
Sc	50	61	41
Co	64	84	53
Pb	18	20	10
Ni	97	163	53
Th	14	15	13
Cr	173	366	89
Rb	4	10	1
V	761	952	506
Zr	47	113	19
Y	17	28	13
Ba	95	117	62
Sr	212	253	173

Table 2. Summary of compositions of starting materials for MLS–2.*

	1	2	3	4	5
$Si-O_2$	49.78	51.45	50.68	43.6	43.9
$Ti-O_2$	0.00	–	0.07	0.1	0.5
Al_2-O_3	29.37	31.94	30.67	34.0	28.8
Fe-O	1.6	tr	0.29	1.5	4.9
Fe_2-O_3	0.34	tr	0.21	0.00†	0.00†
Mn-O	0.08	–	–	–	0.1
Mg-O	1.07	0.27	0.42	1.3	5.7
Ca-O	11.86	14.31	13.79	19.0	15.6
Na_2-O	4.39	0.85	3.40	0.5	0.5
K_2-O	0.46	0.21	0.09	–	0.1
P_2-O_5	–	–	0.16	–	–
H_2-O	1.76	0.68	0.50	0.00†	0.00†
Total	100.71	99.71	100.28	100.0	100.1

Notes: Analyses 1–3 from Grout, F.F., and Schwartz, G.W., 1939, Bulletin 28 Minnesota Geological Survey, table 4, analyses 1, 3, and 7, respectively. These analyses are representative of the range of compositions of starting materials for MLS–2. Analyses 4 and 5 from Taylor, S.R., 1974, Lunar Science: A Post-Apollo View, table 5.4, p. 216, Pergamon. MLS–2 has higher silica, ferric iron, soda, potash, and water than lunar highlands rocks. MLS–2 plasma processed simulant will have compositions within the range of the starting materials but with up to a few percent (of the amount present in the starting materials) lower ferric iron, soda, and much lower water content (~0.05 weight percent) than the starting materials.

*Provided by University of Minnesota Space Science Department.

†Expected values: – not analyzed; tr – < ~ 0.1 weight percent.

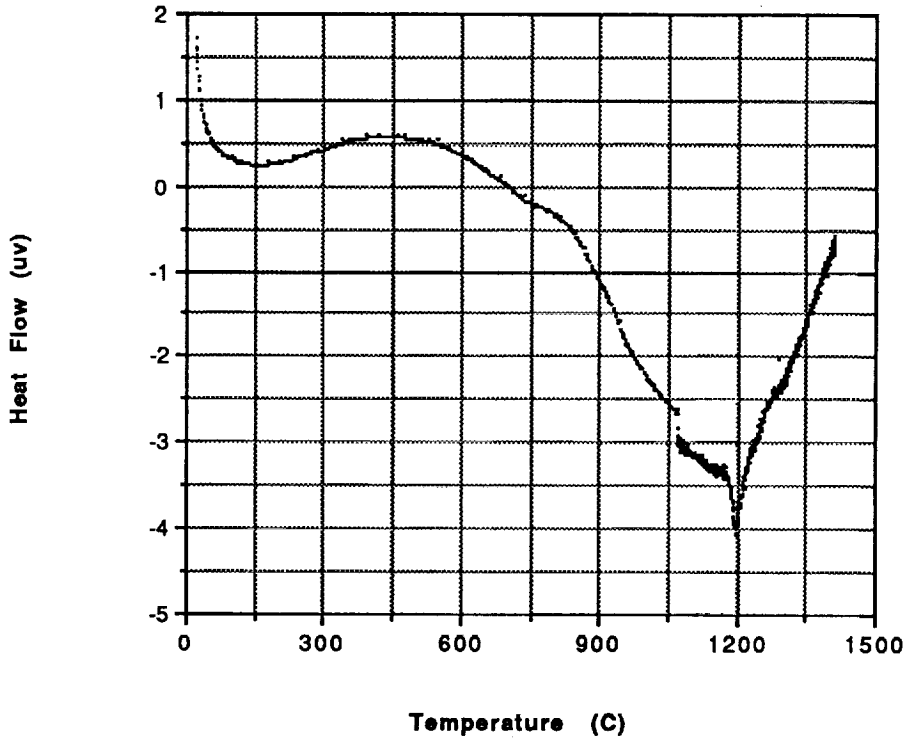

Figure 1. MLS–1 DTA curve.

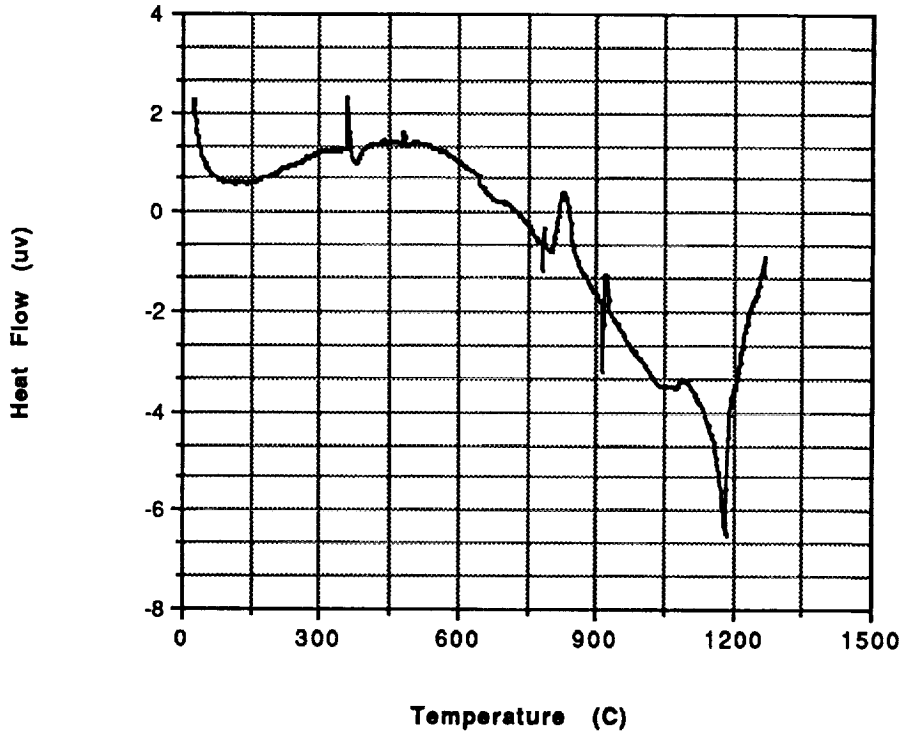

Figure 2. MLS–1 glass DTA curve.

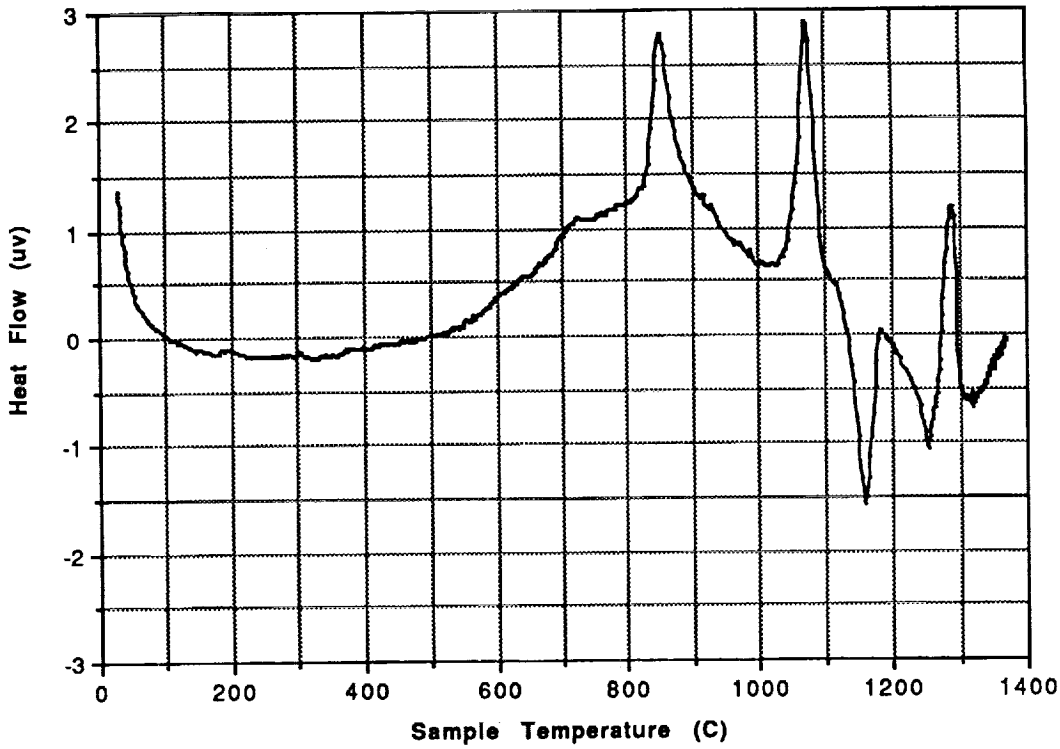

Figure 3. DTA curve for vitrified MLS–2.

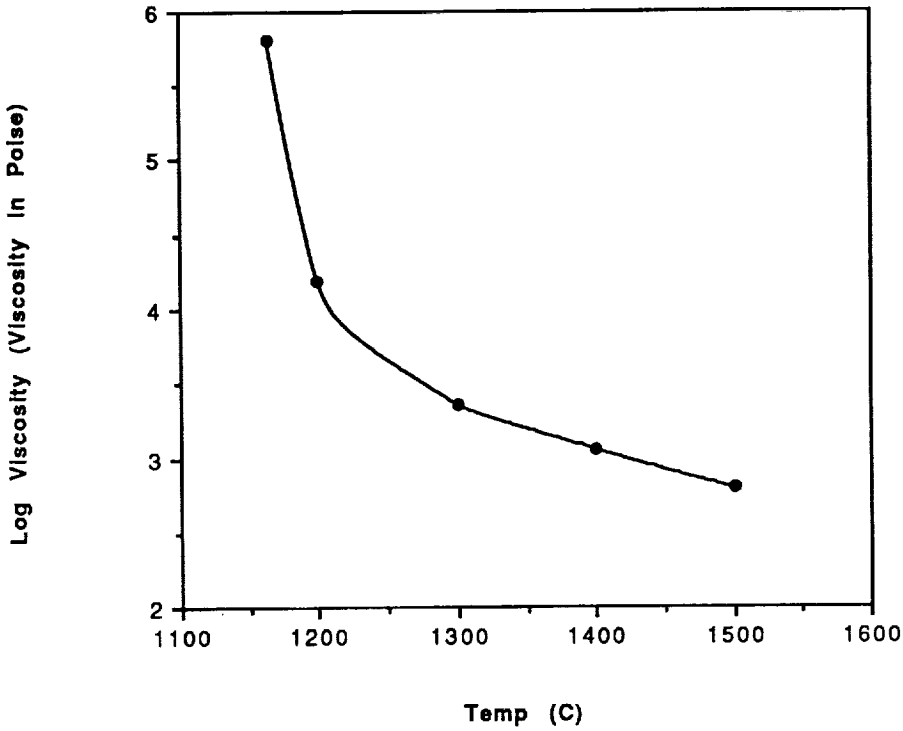

Figure 4. MLS–1 viscosity curve.

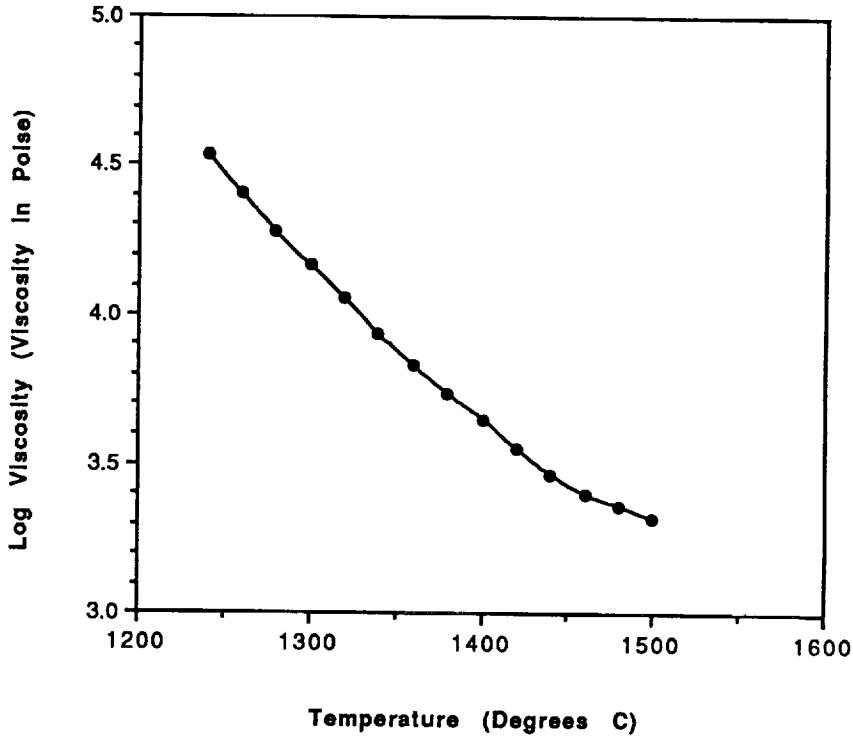

Figure 5. MLS–2 viscosity curve.

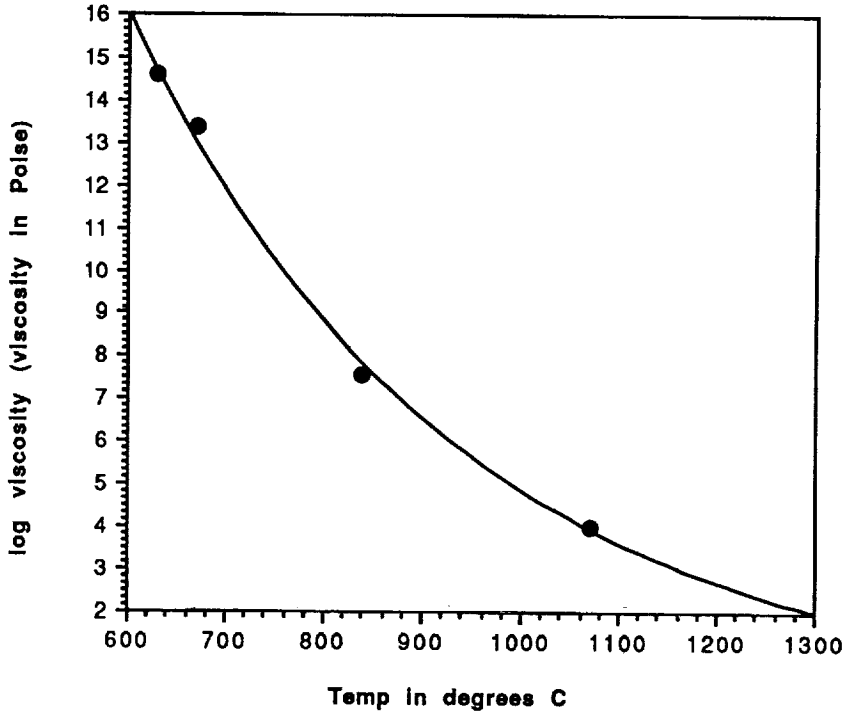

Figure 6. E-glass viscosity curve.

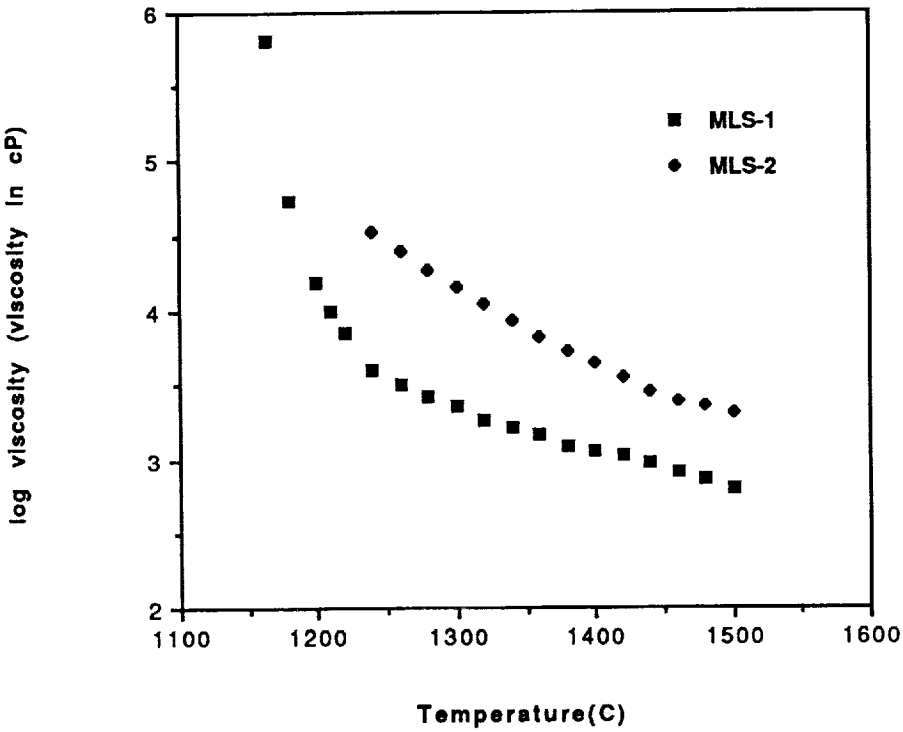

Figure 7. Comparison of MLS–1 and MLS–2 viscosities.

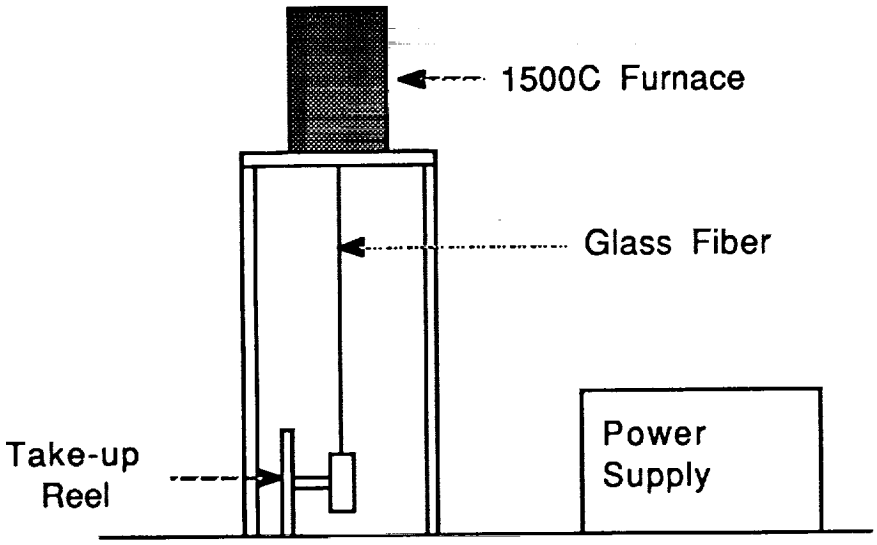

Figure 8. Schematic of laboratory fiber pulling unit.

ORIGINAL PAGE
BLACK AND WHITE PHOTOGRAPH

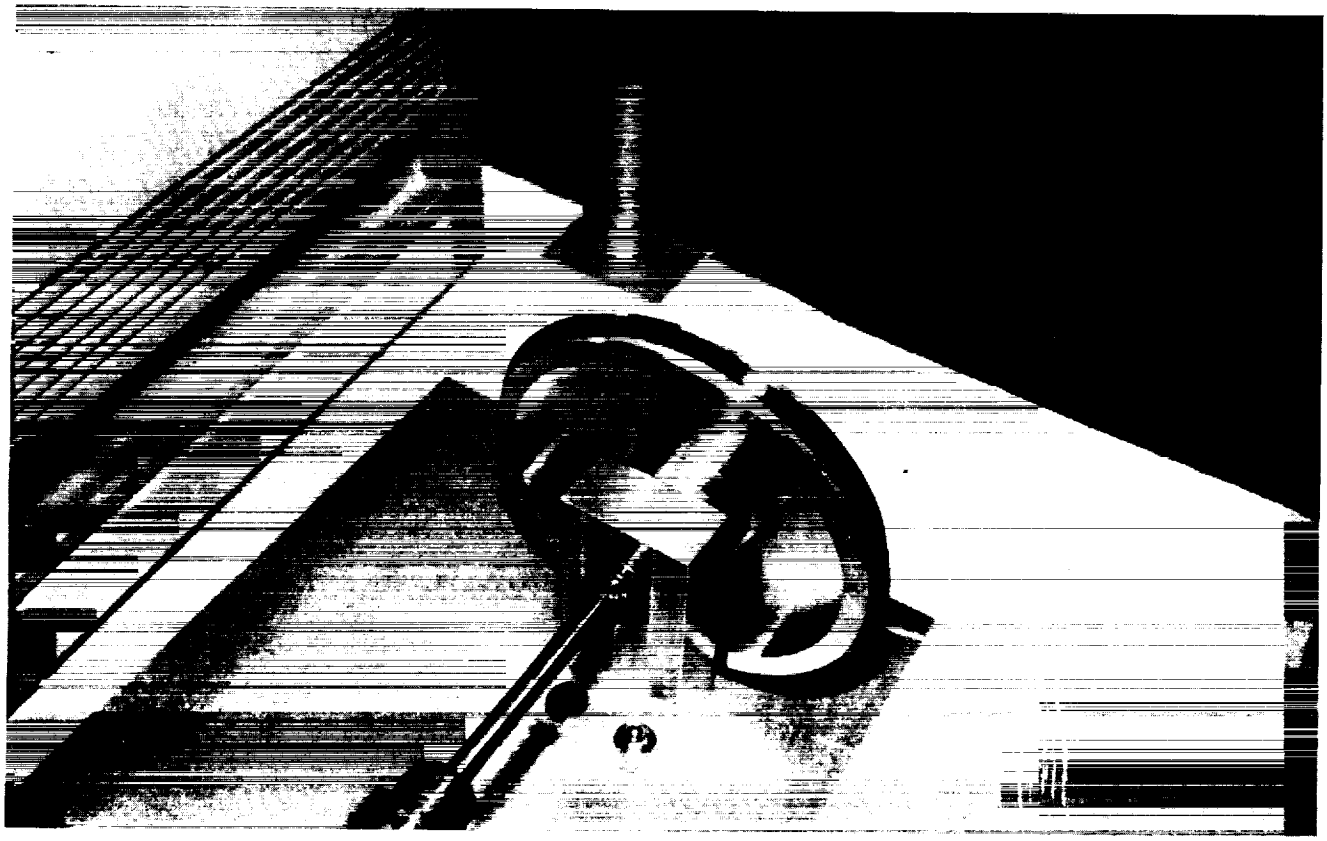

Figure 9. Continuously wound MLS–2 fiber doped with 8 percent B_2-O_3.

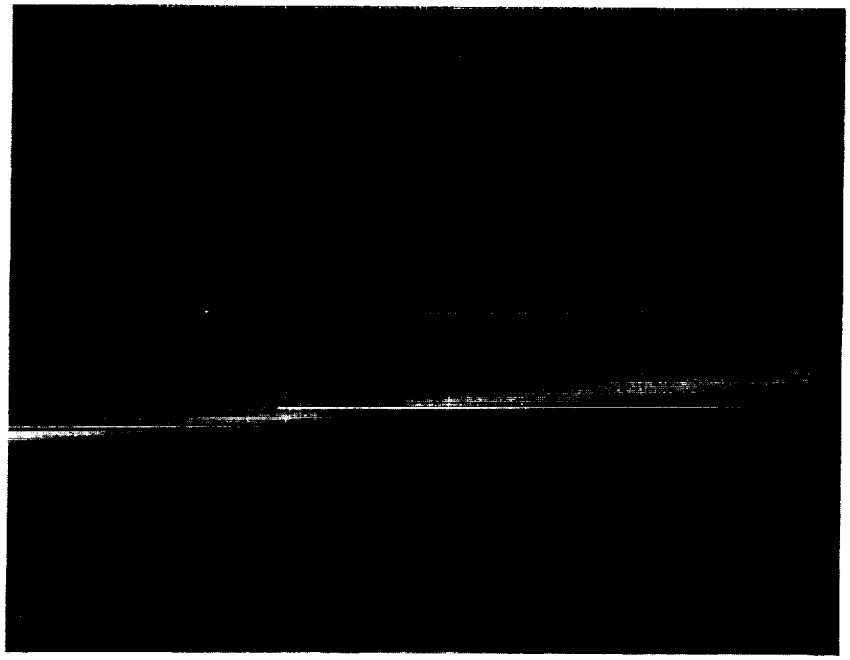

Figure 10. MLS–2 fiber doped with 8 weight percent B_2-O_3. Fiber diameter is 80 microns.

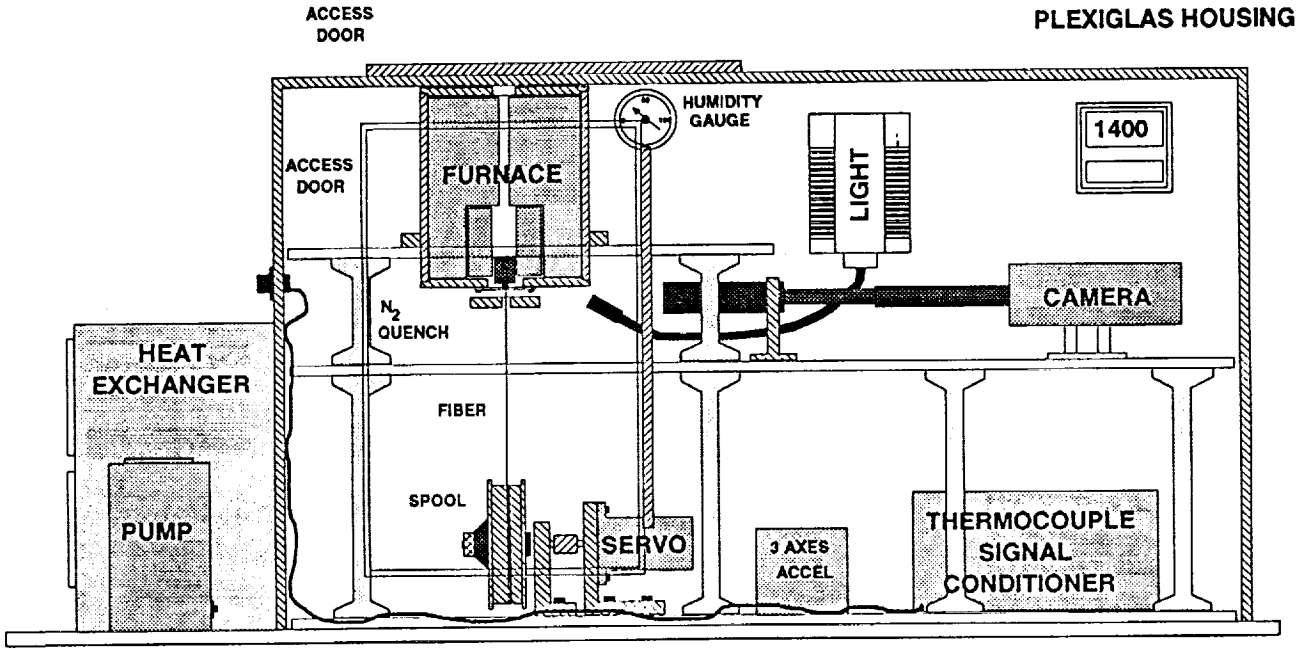

Figure 11. Schematic of FPA.

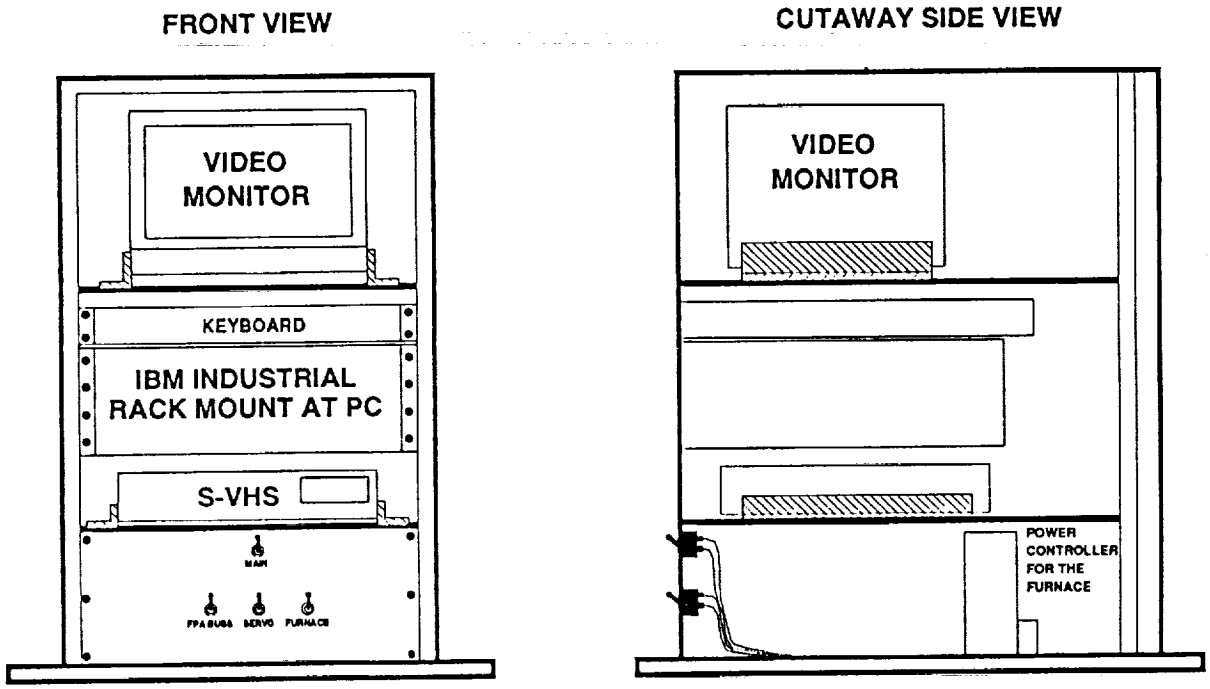

Figure 12. Schematic of FPA data acquisition system.

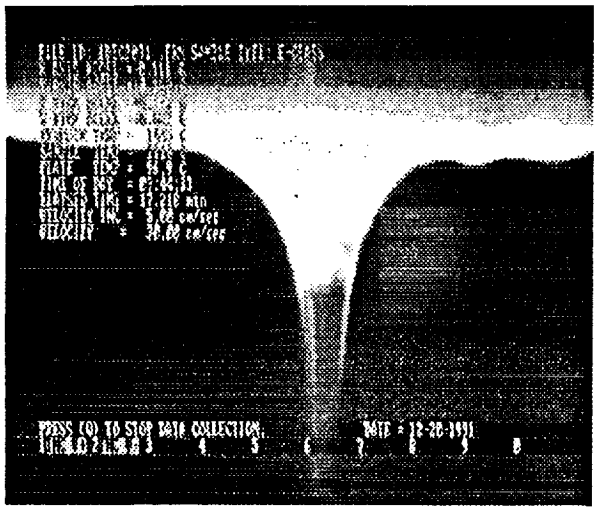

(a) Jet zone during 1/6-g period. Actual g level was 0.167 g.

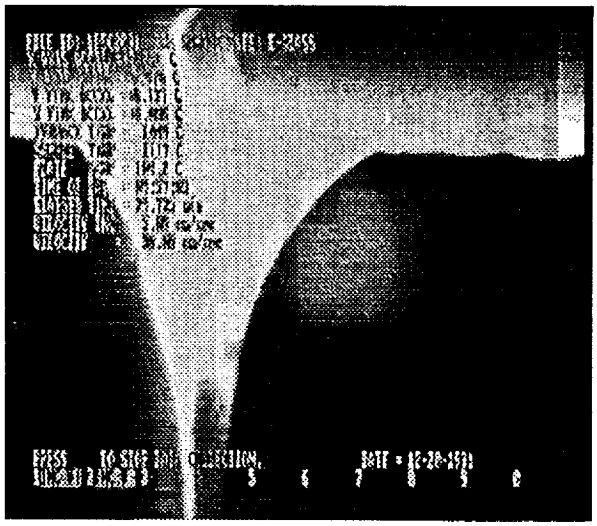

(b) Jet zone during normal g period. Actual g level was 0.985 g.

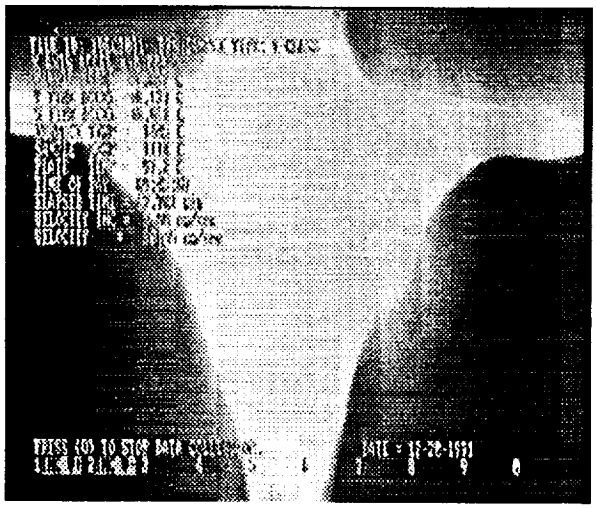

(c) Jet zone during high g period. Actual g level was 1.736 g.

Figure 13. Fiber jet zones during parabolic maneuver.

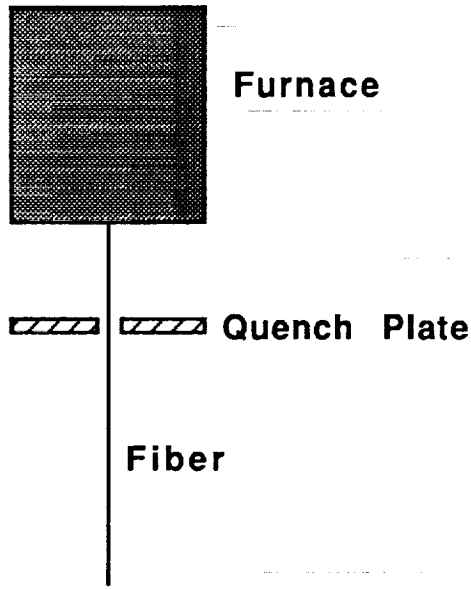

Figure 14. Concept for quenching glass fiber.

APPROVAL

GLASS FIBER PROCESSING FOR THE MOON/MARS PROGRAM

By D.S. Tucker, E. Ethridge, and P. Curreri

The information in this report has been reviewed for technical content. Review of any information concerning Department of Defense or nuclear energy activities or programs has been made by the MSFC Security Classification Officer. This report, in its entirety, has been determined to be unclassified.

R.G. Clinton
Chief, Ceramics and Coatings Branch

C.R. McIntosh
Chief, Nonmetallic Materials Division

P.H. Schuerer
Director, Materials and Processes Laboratory

☆ U. S. GOVERNMENT PRINTING OFFICE 1992 - 733-050/602009

REPORT DOCUMENTATION PAGE

Form Approved
OMB No. 0704-0188

Public reporting burden for this collection of information is estimated to average 1 hour per response, including the time for reviewing instructions, searching existing data sources, gathering and maintaining the data needed, and completing and reviewing the collection of information. Send comments regarding this burden estimate or any other aspect of this collection of information, including suggestions for reducing this burden, to Washington Headquarters Services, Directorate for Information Operations and Reports, 1215 Jefferson Davis Highway, Suite 1204, Arlington, VA 22202-4302, and to the Office of Management and Budget, Paperwork Reduction Project (0704-0188), Washington, DC 20503.

1. AGENCY USE ONLY *(Leave blank)*	2. REPORT DATE	3. REPORT TYPE AND DATES COVERED
	October 1992	Technical Memorandum

4. TITLE AND SUBTITLE

Glass Fiber Processing for the Moon/Mars Program
(Center Director's Discretionary Fund Final Report)

5. FUNDING NUMBERS

6. AUTHOR(S)

D.S. Tucker, E. Ethridge, and P. Curreri

7. PERFORMING ORGANIZATION NAME(S) AND ADDRESS(ES)

George C. Marshall Space Flight Center
Marshall Space Flight Center, Alabama 35812

8. PERFORMING ORGANIZATION REPORT NUMBER

9. SPONSORING/MONITORING AGENCY NAME(S) AND ADDRESS(ES)

National Aeronautics and Space Administration
Washington, DC 20546

10. SPONSORING/MONITORING AGENCY REPORT NUMBER

NASA TM-108379

11. SUPPLEMENTARY NOTES

Prepared by Materials and Processes Laboratory, Science and Engineering Directorate.

12a. DISTRIBUTION/AVAILABILITY STATEMENT

Unclassified — Unlimited

12b. DISTRIBUTION CODE

13. ABSTRACT *(Maximum 200 words)*

Glass fiber has been produced from two lunar soil simulants. These two materials simulate lunar mare soil and lunar highland soil compositions, respectively. Short fibers containing recrystallized areas were produced from the as-received simulants. Doping the highland simulant with 8 weight percent B_2O_3 yielded a material which could be spun continuously. The effects of lunar gravity on glass fiber formation were studied utilizing NASA's KC–135 aircraft. Gravity was found to play a major role in final fiber diameter.

14. SUBJECT TERMS	15. NUMBER OF PAGES
Fiberglass, Lunar Processing, Reduced Gravity	22
	16. PRICE CODE: NTIS

17. SECURITY CLASSIFICATION OF REPORT	18. SECURITY CLASSIFICATION OF THIS PAGE	19. SECURITY CLASSIFICATION OF ABSTRACT	20. LIMITATION OF ABSTRACT
Unclassified	Unclassified	Unclassified	Unlimited